Title
Enhancing Terpene Yield from Sugars via Novel Routes to 1-Deoxy-d-Xylulose 5-Phosphate

Journal
Applied and Environmental Microbiology, 81(1)

ISSN
0099-2240

Authors
Kirby, James
Nishimoto, Minobu
Chow, Ruthie WN
et al.

Publication Date
2015

DOI
10.1128/aem.02920-14

Peer reviewed

AEM
Journals.ASM.org

Enhancing Terpene Yield from Sugars via Novel Routes to 1-Deoxy-D-Xylulose 5-Phosphate

James Kirby,[a,b] Minobu Nishimoto,[a,b] Ruthie W. N. Chow,[a] Edward E. K. Baidoo,[b] George Wang,[b] Joel Martin,[e] Wendy Schackwitz,[e] Rossana Chan,[a] Jeffrey L. Fortman,[a] Jay D. Keasling[a,b,c,d]

California Institute of Quantitative Biosciences (QB3), University of California, Berkeley, Berkeley, California, USA[a]; Joint BioEnergy Institute, Emeryville, California, USA[b]; Department of Chemical and Biomolecular Engineering, University of California, Berkeley, Berkeley, California, USA[c]; Physical Biosciences Division, Lawrence Berkeley National Laboratory, Berkeley, California, USA[d]; Joint Genome Institute, Walnut Creek, California, USA[e]

Terpene synthesis in the majority of bacterial species, together with plant plastids, takes place via the 1-deoxy-D-xylulose 5-phosphate (DXP) pathway. The first step of this pathway involves the condensation of pyruvate and glyceraldehyde 3-phosphate by DXP synthase (Dxs), with one-sixth of the carbon lost as CO_2. A hypothetical novel route from a pentose phosphate to DXP (nDXP) could enable a more direct pathway from C_5 sugars to terpenes and also circumvent regulatory mechanisms that control Dxs, but there is no enzyme known that can convert a sugar into its 1-deoxy equivalent. Employing a selection for complementation of a *dxs* deletion in *Escherichia coli* grown on xylose as the sole carbon source, we uncovered two candidate nDXP genes. Complementation was achieved either via overexpression of the wild-type *E. coli yajO* gene, annotated as a putative xylose reductase, or via various mutations in the native *ribB* gene. *In vitro* analysis performed with purified YajO and mutant RibB proteins revealed that DXP was synthesized in both cases from ribulose 5-phosphate (Ru5P). We demonstrate the utility of these genes for microbial terpene biosynthesis by engineering the DXP pathway in *E. coli* for production of the sesquiterpene bisabolene, a candidate biodiesel. To further improve flux into the pathway from Ru5P, nDXP enzymes were expressed as fusions to DXP reductase (Dxr), the second enzyme in the DXP pathway. Expression of a Dxr-RibB(G108S) fusion improved bisabolene titers more than 4-fold and alleviated accumulation of intracellular DXP.

Terpenes constitute a very large family of natural products, members of which are produced in virtually all free-living organisms (1). The diverse array of structures within the terpene family is reflected by the variety of applications in society, ranging from nutrition (carotenoids) and medicine (artemisinin, paclitaxel [originally taxol]) to industrial materials (isoprene, linalool) and candidate biofuels (farnesene, bisabolene, pinene) (2). Terpenes can be synthesized via either the mevalonate pathway or the 1-deoxy-D-xylulose 5-phosphate (DXP) pathway, the former predominating in the eukaryotic cytosol and the latter in plastids, while prokaryotes may contain either pathway or, in some cases, both pathways (3).

Commercial-scale terpene production has been demonstrated in a variety of organisms, for example, carotenoids (via the DXP pathway) in algae (4, 5), paclitaxel (via DXP) in *Taxus* sp. (6), and artemisinin (via mevalonate) in *Saccharomyces cerevisiae* (7). Key metrics in determining the likelihood of commercial viability, particularly when targeting terpenes valued within the range of commodity chemicals or biofuels, are yield, productivity, and titer (8, 9). Of the two metabolic routes, the DXP pathway is considered the better option from the viewpoint of pathway efficiency—for example, the theoretical maximum yield of isoprene from glucose is around 20% higher when synthesized via DXP instead of mevalonate (9, 10). In considering production of terpenes from hemicellulosic feedstocks, conversion efficiencies of pentoses, predominantly xylose and arabinose, should also be taken into account (11). Although DXP is structurally similar to pentose phosphates, it is synthesized by DXP synthase (Dxs) via condensation of pyruvate and glyceraldehyde 3-phosphate, with a concomitant loss of CO_2. Dxs is a key control point in the pathway and has been found to be regulated at the transcriptional and translational levels as well as being feedback inhibited by the prenyl phosphates (12). We reasoned that a novel route from a pentose phosphate to DXP (nDXP) could have several advantages from a pathway-engineering standpoint, including carbon conservation, avoidance of regulatory mechanisms that target Dxs, and a more direct entry point for pentoses into the terpene biosynthetic pathway. However, to our knowledge there are no 1-deoxy sugars made from sugars in nature, and we therefore decided to employ a directed-evolution strategy.

We report the discovery of two nDXP routes following complementation of a *dxs* deletion in *Escherichia coli* grown on xylose. One of these arose through spontaneous mutations in the native *ribB* coding sequence (cds), normally involved in riboflavin biosynthesis (13). The second route was discovered following overexpression of one of several rationally selected candidate nDXP genes, *yajO*, located next to *dxs* on the *E. coli* chromosome and annotated as a putative xylose reductase, although little evidence has been found to support this proposed function (14). Both

Received 5 September 2014 **Accepted** 9 October 2014

Accepted manuscript posted online 17 October 2014

Citation Kirby J, Nishimoto M, Chow RWN, Baidoo EEK, Wang G, Martin J, Schackwitz W, Chan R, Fortman JL, Keasling JD. 2015. Enhancing terpene yield from sugars via novel routes to 1-deoxy-D-xylulose 5-phosphate. Appl Environ Microbiol 81:130–138. doi:10.1128/AEM.02920-14.

Editor: R. E. Parales

Address correspondence to Jay D. Keasling, keasling@berkeley.edu.

Supplemental material for this article may be found at http://dx.doi.org/10.1128/AEM.02920-14.

doi:10.1128/AEM.02920-14

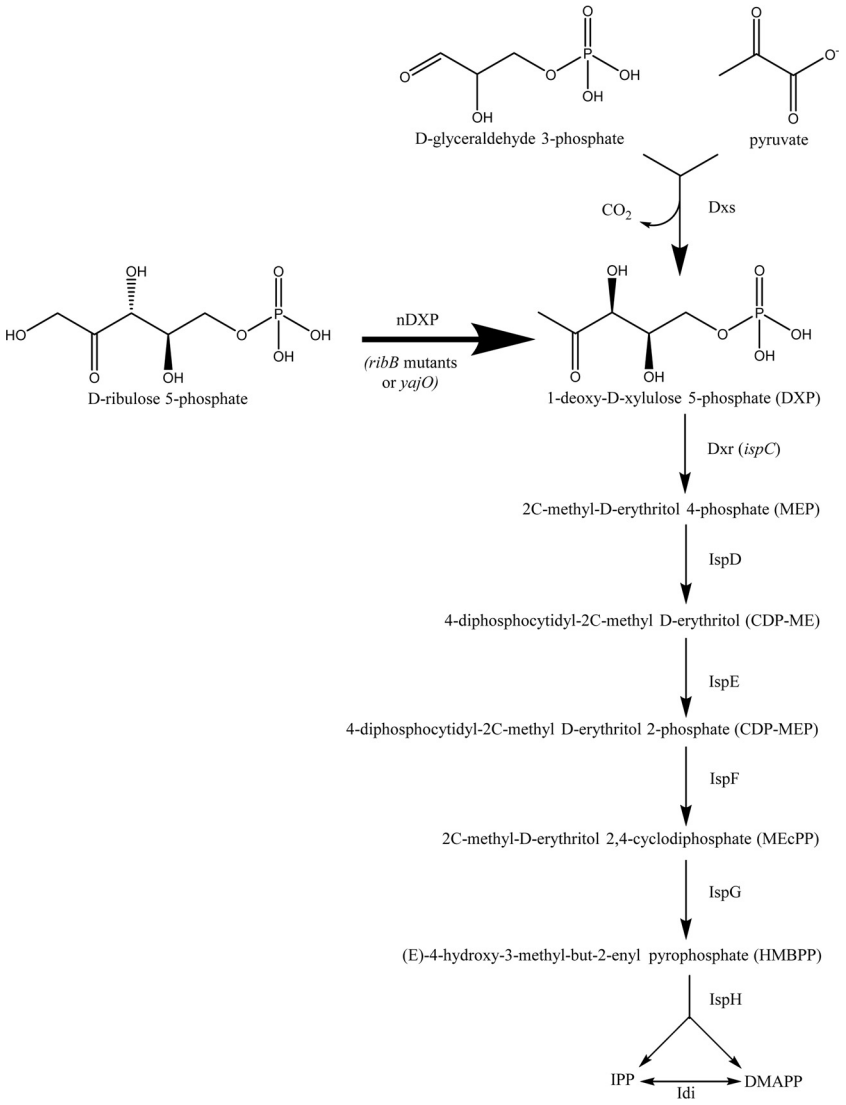

FIG 1 The DXP pathway, together with the alternative nDXP route from Ru5P. IPP, isopentenyl pyrophosphate; DMAPP, dimethylallyl pyrophosphate.

nDXP enzymes were found to catalyze conversion of ribulose 5-phosphate (Ru5P) to DXP, providing a direct route from pentoses to terpenes (Fig. 1).

In order to test the utility of the nDXP genes for terpene production in *E. coli*, we engineered a strain for production of the sesquiterpene bisabolene, a biofuel candidate, by overexpression of pathway enzymes previously found to be limiting. Coexpression of the nDXP genes enhanced bisabolene production 2- to 3-fold, while translational fusions to the succeeding pathway enzyme, DXP reductase (Dxr), increased production up to 4.3-fold.

MATERIALS AND METHODS

Generation of an *E. coli dxs* knockout. To permit deletion of *dxs*, *E. coli* MG1655 was first transformed with plasmid pMBI (15), harboring four genes (*ERG12* [mevalonate kinase], *ERG8* [phosphomevaloante kinase], and *MVD1* [mevalonate pyrophosphate decarboxylase], all from *Saccharomyces cerevisiae*, and *idi* [isopentenyl pyrophosphate {IPP} isomerase], from *E. coli*) that enable biosynthesis of the isoprenoid precursors IPP and DMAPP when mevalonate is supplied exogenously to cells. Following transformation with pMBI, λ Red recombinase was used to replace the *dxs* cds with a kanamycin marker cassette (16), generating strain Δ*dxs*MB (Table 1). After selection on kanamycin, deletion of *dxs* was confirmed by several diagnostic PCRs, together with verification of mevalonate auxotrophy.

Use of selective pressure to isolate spontaneous nDXP mutants. Subculturing of strain Δ*dxs*MB was carried out in EZ Rich medium (Teknova, Hollister, CA, USA) containing 1% D-xylose (Sigma-Aldrich) as the carbon source (EZ-X). Selective pressure was applied by reducing the concentration of mevalonate (Sigma-Aldrich) from 1.0 mM to 0.1 mM over the course of three cultures (subcultured at mid-log phase; 1/1,000 dilution) and thereafter maintaining mevalonate at 0.1 mM. At each subculture, aliquots containing approximately 10^9 cells were plated onto EZ-X agar lacking mevalonate. Colonies were initially ranked in order of size and further prioritized based on growth in liquid medium lacking mevalonate and containing either glucose or xylose.

Genome sequencing of mevalonate-independent Δ*dxs*MB strains. Strains isolated under selective pressure that grew well in the absence of mevalonate were submitted to the Joint Genome Institute (JGI) for genome sequencing, using the parent Δ*dxs*MB strain as a reference. Libraries were generated from 1 μg of genomic DNA using a modified version of Illumina's standard protocol (Illumina Inc., Hayward, CA, USA). DNA

TABLE 1 Primers used in this study

Target gene	Primer name	Primer sequence
dxs knockout[a]	Dxs-KO-f	ATGAGTTTTGATATTGCCAAATACCCGACCCTGGCACTGGTCGACTCCACGTGTAGGCTGGAGCTGCTTCG
	Dxs-KO-r	TTCTACGGTGACCAGCGCTTCATGGCTGGCGGCCATTTCCAGAATTAACGATGGGAATTAGCCATGGTCC
ribB	pTrc-ribB-f	GACCATGGCAAATCAGACGCTACTTTCCTCTTTTGGTACG
	pTrc-ribB-r	CCAAGCTTTCAGCTGGCTTTACGCTCATGTGCGTGAC
yajO[b]	pTrc-yajO-f	AACCATGGAACAATACAACCCCTTAGGAAAAACC
	pTrc-yajO-r	AAAAGCTTTTATTTAAATCCTACGACAGGATGCG
rib	pTrc-ribB-S-f	GACCATGGCAAATCAGACGCTACTTTCC
rib StrepII tag	pTrc-ribB-S-r	TTAAGCTTTCA*TTTTTCAAACTGCGGATGGCTCCA*GCTGGCTTTACGCTCATGTGCC
yajO	pTrc-yajO-S-f	ACATCGATGCAATACAACCCCTTAGGA
yajO StrepII tag	pTrc-yajO-S-r	TTAAGCTTTTA*TTTTTCAAACTGCGGATGGCTCCA*TTTAAATCCTACGACAGGATGCG
AgBIS gene	pBbA1k-BIS-f	AAGAATTCAGTTTTTCCCTACTAGTTCAGGAGGTATTCATGGCGGGTGTTTCTGCGGTTTCTAAAGTTTCTTCTCTGG
	pBbA1k-BIS-r	TTGGATCCTTACAGCGGCAGCGGTTCGATCAGGCA
ispA[c]	pBbA1k-ispA-f	AAGGATCCTCTAGAGGAGGTACACTATGGACTTTCCGCAGCAACTCGAAGC
	pBbA1k-ispA-r	AACTCGAGTTATTTATTACGCTGGATGATGTAG
ispDF[d]	pBbA1k-ispDF-f	CGCTGCCGCTGTAAGGATCCCCCGGGAATTAACATGGCAA
	pBbA1k-ispDF-r	CATAATTTCTCACATGTAATTCATTTTGTTGCCTTAATGAGTAGC
idi[d]	pBbA1k-idi-f	TCATTAAGGCAACAAAATGAATTACATGTGAGAAATTATGC
	pBbA1k-idi-f	CCTGGAGATCCTTACTCGAGTTATTTAAGCTGGGTAAATG
yajO-ispC[e]	Ptrc-yajO-F-f	GAATTGTGAGCGGATAACAATTTCACACAGGAAACAGACCATGACTGGGGTGAACGAATGCAG
	ispC-GP-f	AAACCGCATCCTGTCGTAGGATTTAAA**GGTCCAGGCCC**TAAGCAACTCACCATTCTGGGCT
	yajO-GP-r	CGGTCGAGCCCAGAATGFGTGAGTTGCTT**AGGGCCTGGACC**TTTAAATCCTACGACAGGATGCGGTTT
	ispC-PT-f	CCTGTCGTAGGATTTAAA**CCAACACCAACGCCAACGACACCAACTCCAACA**AAGCAACTCACCATTCTGGGC
	yajO-PT-r	AGAATGGTGAGTTGCTT**TGTTGGAGTTGGTGTCGTTGGCGTTGGTGTTGG**TTTAAATCCTACGACAGGATGCGGTT
	ispC-Ptrc-r	GGCTGAAAATCTTCTCTCATCCGCCAAAACAGCCAAGCTTTCAGCTTGCGAGACGCATCAC
ribB-ispC[e]	Ptrc-ribB-F-f	GAATTGTGAGCGGATAACAATTTCACACAGGAAACAGACCATGGCAAATCAGACGCTACTTTCCTCTTTT
	IspC-G2-F-f	CGTCAGGCACATGAGCGTAAAGCCAGC**GGTTCTGGCGGTTCCGGT**AAGCAACTCACCATTCTGGGCT
	ribB-G2-r	GAGCCGGTCGAGCCCAGAATGGTGAGTTGCTT**ACCGGAACCGCCAGAACC**GCTGGCTTTACGCTCATGTGCCTG
	ispC-GP-F-f	CCGTCAGGCACATGAGCGTAAAGCCAGC**GGTCCAGGCCCT**AAGCAACTCACCATTCTGGGCTCG
	ribB-GP-r	GAGCCGGTCGAGCCCAGAATGGTGAGTTGCTT**AGGGCCTGGACC**GCTGGCTTTACGCTCATGTGCCTGA
	ispC-Ptrc-r	GGCTGAAAATCTTCTCTCATCCGCCAAAACAGCCAAGCTTTCAGCTTGCGAGACGCATCAC
ispC-yajO[e]	ispC-Ptrc-f	GAATTGTGAGCGGATAACAATTTCACACAGGAAACAGACCATGAAGCAACTCACCATTCTGGGCT
	IspC-G2-r	GGCTGCATTCGTTCACCCCAGT**ACCGGAACCGCCAGAACC**GCTTGCGAGACGCATCACCTCTTTT
	yajO-G2-f	AGGTGATGCGTCTCGCAAGC**GGTTCTGGCGGTTCCGGT**ACTGGGGTGAACGAATGCAGC
	yajO-Ptrc-r	GGCTGAAAATCTTCTCTCATCCGCCAAAACAGCCAAGCTTTTATTTAAATCCTACGACAGGATGCGGTTTATACG
ispC-ribB[e]	IspC-Ptrc-f	GAATTGTGAGCGGATAACAATTTCACACAGGAAACAGACCATGAAGCAACTCACCATTCTGGGCT
	IspC-G2-R-r	AAAAGAGGAAAGTAGCGTCTGATTTGC**ACCGGAACCGCCAGAACC**GCTTGCGAGACGCATCACCTC
	ribB-G2-f	TGATGCGTCTCGCAAGC**GGTTCTGGCGGTTCCGGT**GCAAATCAGACGCTACTTTCCTCTTTTGG
	ribB-Ptrc-r	GGCTGAAAATCTTCTCTCATCCGCCAAAACAGCCAAGCTTTCAGCTGGCTTTACGCTCATGTGC

[a] The 50 nucleotides (nt) at the 5′ end of the primers match the ends of the *dxs* cds, while the underlined sequence matches the kanamycin resistance cassette. The kanamycin marker cassette was amplified by PCR from plasmid pDK13 (16) using the primers listed. *E. coli* MG1655 harboring pMBI was transformed with this PCR product together with the pKD46 plasmid, containing the gene for γ Red recombinase (16). Following selection on LB-kanamycin, deletion of *dxs* was confirmed by several diagnostic PCRs, and loss of the temperature-sensitive pDK46 plasmid was facilitated by growth at 37°C.

[b] The *yajO* cds was selected according to the GenBank annotation for *E. coli* MG1655, beginning with the amino acid sequence MQYN. However, the *yajO* sequence in *E. coli* H736 is annotated to contain an additional 14 N-terminal amino acids (beginning MTGV) and the corresponding region in MG1655 forms a contiguous open reading frame (ORF), but with a putative valine start codon (reading VTGV). Since it is uncertain whether translation of the MG1655 *yajO* cds begins at the annotated Met or at the Val codon 14 amino acids upstream, we overexpressed both versions in the Δ*dxs*MB strain (but substituting Met for Val in the longer version) and found that they both complemented the *dxs* knockout.

[c] The *ispA* cds (encoding FPP synthase) was amplified from *E. coli* MG1655 genomic DNA and cloned between the BamHI and XhoI sites of pBbA1k-AgBIS to make plasmid pBbA1k-AgBIS-*ispA* (pBbA1k-AF).

[d] The *ispDF* operon and *idi* gene were amplified from *E. coli* MG1655 genomic DNA and cloned between the BamHI and XhoI sites of pBbA1k-AgBIS using SLIC to make plasmid pBbA1k-AgBIS-*ispDF-idi* (pBbA1k-Aii). Sequences homologous to each other or to the vector backbone are underlined. This fragment was subsequently cloned into the XhoI site of pBbA1k-AgBIS-*ispA* to make plasmid pBbA1k-AgBIS-*ispA-ispDF-idi* (pBbA1k-AFii).

[e] nDXP-Dxr fusions were constructed by the use of PCR splicing by overlap extension (SOE). Three fusions for *yajO-ispC* and three fusions for *rib-ispC* were constructed and cloned between the NcoI and HindIII sites of pTrc99A using SLIC. Nucleotides encoding fusion linkers (GP, GPGP; PT, PTPTPTTPTPT; G2, GSGGSG) are shown in bold.

was sheared using a sonicator (Covaris, Inc., Wolburn, MA, USA) to generate fragments of 200 to 800 bp in length, and the fragments were then size selected by solid-phase reversible immobilization (SPRI) (Beckman Coulter, Indianapolis, IN, USA) to around 300 bp. Selected fragments were end repaired, phosphorylated, and A-tailed using the polymerase activity of the Klenow fragment of *E. coli* DNA polymerase I and then ligated with Illumina paired-end sequencing adapters and amplified by 10 cycles of PCR. The prepared sample libraries were quantified using a Kapa next-generation sequencing library quantitative PCR (qPCR) kit (Kapa Biosystems, Wolburn, MA, USA) and run on a LightCycler 480 real-time PCR instrument (Roche, Pleasanton, CA, USA). The libraries of quantified samples were then prepared for sequencing on the Illumina sequencing platform utilizing a paired-end cluster generation kit, v4, and Illumina's cBot instrument to generate clustered flow cells for sequencing. Sequencing of the flow cells was performed on an Illumina GAIIx sequencer using SBS sequencing kits, v4, following a program employing 2 sets of 36 runs.

Generation of additional *ribB* mutants. To screen for additional *ribB* mutations that complement Δ*dxs*, two approaches were taken: chemical mutagenesis by hydroxylamine (Sigma-Aldrich) and error-prone PCR (EP-PCR) mutagenesis. Hydroxylamine mutagenesis was performed as described previously (17) except that DNA was cleaned up using a QIAquick PCR purification kit (Qiagen, Valencia, CA, USA). EP-PCR mutagenesis was performed using the Clontech Diversify approach (Clontech, Mountain View, CA, USA) and conditions 2 and 5 in the manufacturer's protocol, predicted to generate 2.3 and 4.6 mutations per kb, respectively. The *ribB* cds was cloned between the NcoI and HindIII sites of pTrc99A under the control of the isopropyl-β-D-thiogalactopyranoside (IPTG)-inducible trc promoter (Table 1). Mutant libraries were transformed into strain Δ*dxs*MB and grown under selective pressure as described above except that 50 μM IPTG (Calbiochem/EMD Millipore, Billerica, MA, USA) was included in media to induce *ribB* expression. Plasmids were recovered from mevalonate-independent strains, which were isolated from EZ-X agar plates and ranked in order of growth, and the *ribB* cds was sequenced.

Expression of other candidate nDXP genes. Several genes or gene combinations were investigated for their ability to complement a *dxs* knockout, and overexpression of one of these candidates, *yajO* from *E. coli*, enabled mevalonate-independent growth. The *yajO* cds was cloned between the NcoI and HindIII sites of pTrc99A (Table 1) and transformed into strain Δ*dxs*MB, and the resulting strain was then grown under selective pressure in the presence of 50 μM IPTG. EP-PCR mutagenesis of *yajO* was carried out as described for *ribB* above.

***In vitro* analysis of RibB(G108S) and YajO.** Coding sequences for RibB(G108S) and YajO were amplified by PCR using reverse primers that added sequence encoding C-terminal StrepII peptide tags ([WSHPQFEK]) and cloned into pTrc99A (Table 1). Protein was expressed in *E. coli* BLR(DE3) grown in LB medium containing 100 μM IPTG and purified using a StrepTactin SpinPrep kit (EMD Millipore). Protein purity was determined to be around 95% by SDS-PAGE, and protein was directly used for assays. *In vitro* reactions were carried out by combining 13.2 μg purified protein and 5 mM substrate in assay buffer (50 mM TrisCl [pH 7.5], 150 mM NaCl, 10 mM $MgCl_2$, 5 mM dithiothreitol [DTT]) and incubating at 37°C for 30 min (18). Following addition of methanol (high-performance liquid chromatography [HPLC] grade; Sigma-Aldrich) to reach a concentration of 50% (vol/vol), samples were analyzed by liquid chromatography-mass spectrometry (LC-MS) alongside a DXP standard (Echelon Inc., Salt Lake City, UT, USA). Chromatographic separation was achieved using an Agilent 1200 Rapid Resolution HPLC system and the hydrophilic interaction liquid chromatography (HILIC) method from Baidoo et al. (19), and metabolites were detected by the use of an Agilent 6210 TOF MS system as described previously (20).

Terpene biosynthesis in *E. coli*. Amorphadiene production levels were compared using the original Δ*dxs*MB parent strain and an equivalent strain harboring a single mutation encoding RibB(G92D). Strains were transformed with the pADS plasmid, encoding amorphadiene synthase from *Artemisia annua* (15), and grown at 37°C in M9 medium (Sigma-Aldrich) containing 1% xylose, 0.5 mM IPTG, and a 10% (vol/vol) dodecane (Sigma-Aldrich) overlay (to capture amorphadiene), with or without 5 mM mevalonate. Amorphadiene production was measured by gas chromatography-mass spectrometry (GC-MS) as described previously (21).

Bisabolene production was tested in *E. coli* BL21(DE3) harboring a plasmid containing an nDXP gene, or containing *rfp* (encoding red fluorescent protein [RFP]) as a control, and a second plasmid harboring the *Abies grandis* bisabolene synthase (AgBIS) gene, amplified from pRSLeu2d-BISopt (22), coupled with *E. coli* DXP pathway genes *ispD*, *ispF*, and *idi* (Fig. 1; see Table 1 for cloning details). The nDXP genes were expressed on pTrc99A plasmids as described above, while the AgBIS and the DXP pathway genes were expressed on pBbA1k (23). Strains were grown at 37°C in EZ-X medium containing a 20% (vol/vol) dodecane overlay to an optical density at 600 nm (OD_{600}) of around 1.0, at which point IPTG (200 μM) was added and growth was continued at 30°C; bisabolene was measured by GC-MS as described previously (22).

Vectors encoding translation fusions between Dxr (encoded by the *E. coli ispC* gene) and either RibB(G108S) or YajO were constructed using the sequence-and-ligation-independent-cloning (SLIC) approach (24). A combination of fusions was made with Dxr located at either the N or the C terminus and employing peptide linker G2 (GSGGSG), GP (GPGP), or PT (PTPTPTTPTPT) (Table 1). Fusions were expressed on pTrc99A plasmids, while the AgBIS gene combined with *E. coli* DXP pathway genes *ispD*, *ispF*, *idi*, and/or *ispA* was expressed on pBbA1k. Strains were grown in EZ-X medium and bisabolene levels quantified as described above.

Quantification of DXP pathway intermediates. DXP pathway intermediates were extracted from *E. coli* by brief centrifugation (3,000 × *g* for 3 min at room temperature) of each 5-ml culture, removal of medium, addition of 1 ml ice-cold 50% (vol/vol) methanol (in water) to the cell pellet, vortex mixing for 1 min, centrifugation (15,000 × *g* for 10 min at 4°C), and removal of high-molecular-weight (MW) material from the supernatant by centrifugation (14,000 × *g* for 45 min at 4°C) through a 3,000-MW-cutoff (MWCO) Amicon Ultra 0.5-ml filter (Millipore, Carrigtwohill, Cork, Ireland). Separation of DXP pathway intermediates and quantification using authentic standards (Echelon Inc.) were performed using LC-MS as described above.

RESULTS

Use of selective pressure to isolate spontaneous nDXP mutations. The Δ*dxs*MB strain was constructed to screen for nDXP routes by transforming *E. coli* MG1655 with the pMBI plasmid and deletion of the *dxs* gene. pMBI, which encodes the lower half of the mevalonate pathway, enables growth of strain Δ*dxs*MB in the presence of exogenously supplied mevalonate. A selection for spontaneous nDXP mutants was carried out by subculturing in defined medium containing xylose (EZ-X), coupled with reduction of the mevalonate concentration to growth-limiting levels. Aliquots of each subculture were plated on EZ-X agar lacking mevalonate, and colonies were picked for further analysis. Since mutations in the native *aceE* gene have been reported to complement a *dxs* knockout (25), the *aceE* gene was sequenced in the first 50 isolates, but no mutations were found.

Sequencing of mevalonate-independent Δ*dxs*MB strains. The genomes of eight strains that were isolated at the beginning of the selection process were sequenced, and all were found to have a single nucleotide mutation in the *ribB* gene, namely, S89R (three isolates), G92D (three isolates), or T106I (two isolates). The wild-type RibB enzyme is responsible for synthesis of the riboflavin precursor 3,4-dihydroxy-2-butanone 4-phosphate (DHBP) from Ru5P (13, 26). We also sequenced the genomes of four strains

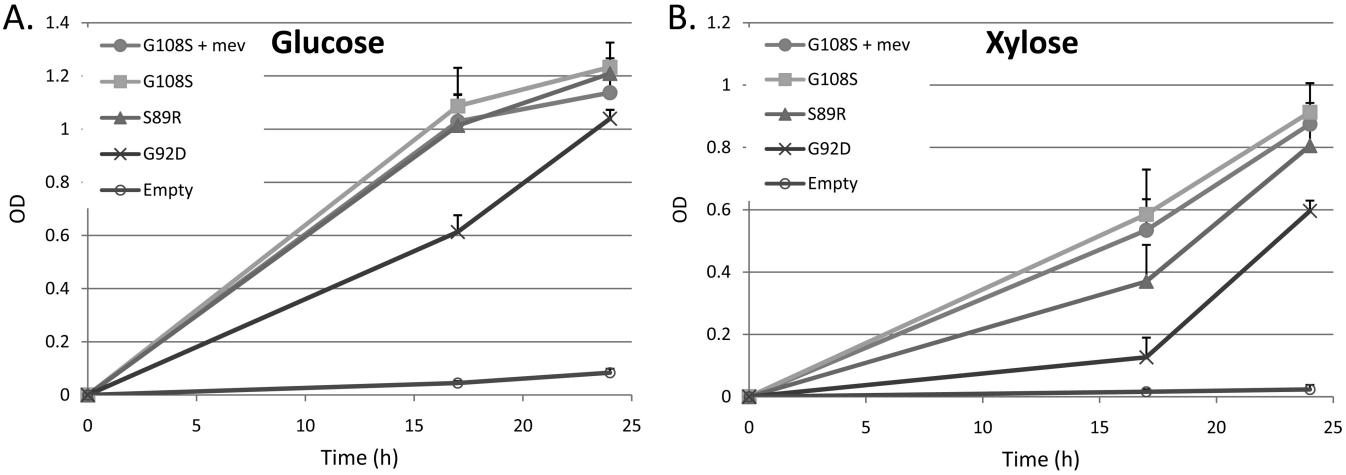

FIG 2 Growth of *E. coli* Δ*dxs*MB expressing various *ribB* mutants on pTrc99A on glucose (A) or xylose (B) as the sole carbon source. Supplementation of the RibB(G108S) strain with 1 mM mevalonate made no significant difference in the growth rate. The Δ*dxs*MB strain harboring an empty vector exhibited minimal growth within 24 h.

isolated at the end of the screening process (following 3 weeks of subculturing under selective pressure), and all three were found to harbor mutations in the *gatC* gene, encoding D296A. GatC functions as a galactitol phosphotransferase permease and has also been found to contribute to xylose uptake (27, 28). Since the strains harboring *ribB* mutations had grown considerably faster than those harboring *gatC* mutations on EZ-X agar lacking mevalonate (3 versus 6 days, respectively), the RibB mutants were investigated further as the most promising nDXP candidates.

Generation of additional *ribB* mutants. Following chemical and EP-PCR mutagenesis of the *ribB* cds, mutant libraries were constructed in pTrc99A and transformed into strain Δ*dxs*MB. Selection in EZ-X was carried out as before, and the 44 fastest-growing isolates were sequenced and found to comprise five discrete mutations: G108S, T88I, V109I, M182I, and G92D (see Table S1 in the supplemental material). A total of 16 mutants that formed colonies within the first 24 h were represented by two mutations, G108S and T88I. The efficiencies of complementation of Δ*dxs* by three of the *ribB* mutants were compared by expression on pTrc99A in strain Δ*dxs*MB and culturing in the absence of mevalonate in either EZ-X or EZ-G (EZ-Rich medium containing 1% D-glucose) (Fig. 2). Expression of *ribB*(G108S) facilitated growth on either glucose or xylose in the absence of mevalonate at rates similar to those seen in media containing mevalonate. The growth rate of the *ribB*(G92D) strain was appreciably lower, while negligible growth was observed in the strain containing an empty vector.

Rational selection of candidate nDXP genes. We selected candidate genes from several species on the basis of genetic or biochemical evidence of possible connections to both C_5 sugars and DXP and investigated their capacity to complement a *dxs* knockout. One of these genes, *yajO* from *E. coli*, was found to support growth on EZ-X agar in the absence of mevalonate when overexpressed in strain Δ*dxs*MB. Two lines of evidence had led to the selection of *yajO*, originally annotated to encode a putative xylose reductase, as a candidate nDXP gene. First, *yajO* was identified in a screen for genes linked to thiamine biosynthesis that employed growth-inhibiting thiamine analog precursors (29). Although the mechanism for resistance to these analogs has not been elucidated, one of the possibilities is increased synthesis of DXP, a precursor to thiamine. Second, *yajO* and the isoprenoid biosynthetic genes *dxs* and *ispA* (the latter encodes farnesyl pyrophosphate synthase) comprise an operon in the genomes of *E. coli* and related species.

Colony formation for strain Δ*dxs*MB harboring pTrc99A-*yajO* on EZ-X agar plates lacking mevalonate usually took 4 to 5 days. Efforts to make this route more efficient through mutagenesis of *yajO* followed by mevalonate selective pressure were unsuccessful. In addition, growth in defined media lacking mevalonate was observed when xylose but not glucose was provided as the sole carbon source (see Fig. S1 in the supplemental material).

Reactions catalyzed by RibB(G108S) and YajO. To elucidate the reactions catalyzed by the nDXP enzymes, RibB(G108S) and YajO containing C-terminal StrepII tags were overexpressed in *E. coli* and purified. *In vitro* assays were conducted using candidate substrates xylose, xylulose, xylulose 5-phospate, and Ru5P, followed by analysis by LC-MS for potential products DXP and 1-deoxy-D-xylulose (DX). Production of DX was considered a possible nDXP route, since DX can be phosphorylated to DXP by the endogenous *E. coli* xylulokinase XylB (30). In the case of both enzymes, DXP was detected only when Ru5P was included as the substrate (Fig. 3). The addition of a cofactor, NADH, NADPH, or ATP, to the reaction mixtures (at 1 mM) did not yield an increase in DXP levels, and no product was detected when the wild-type RibB enzyme was used instead of RibB(G108S) (data not shown).

Utility of nDXP routes for terpene production in *E. coli*. The use of an nDXP route for isoprenoid production was initially evaluated by transforming strain Δ*dxs*MB harboring a genomic *ribB*(G92D) mutation and the corresponding parent strain with pADS, encoding amorphadiene synthase from *A. annua* (15). As expected, growth and amorphadiene production were negligible in the parent strain in the absence of mevalonate whereas the corresponding *ribB*(G92D) strain grew normally and generated 2 mg/liter amorphadiene (see Fig. S2 in the supplemental material). When supplemented with 5 mM mevalonate, strains grew to equivalent ODs, but the amorphadiene titer (5.4 mg/liter or 17 mg/g dry cell weight [DCW]) was over 4-fold higher in the *ribB*(G92D) mutant than in the control strain.

In order to evaluate the use of nDXP enzymes for terpene path-

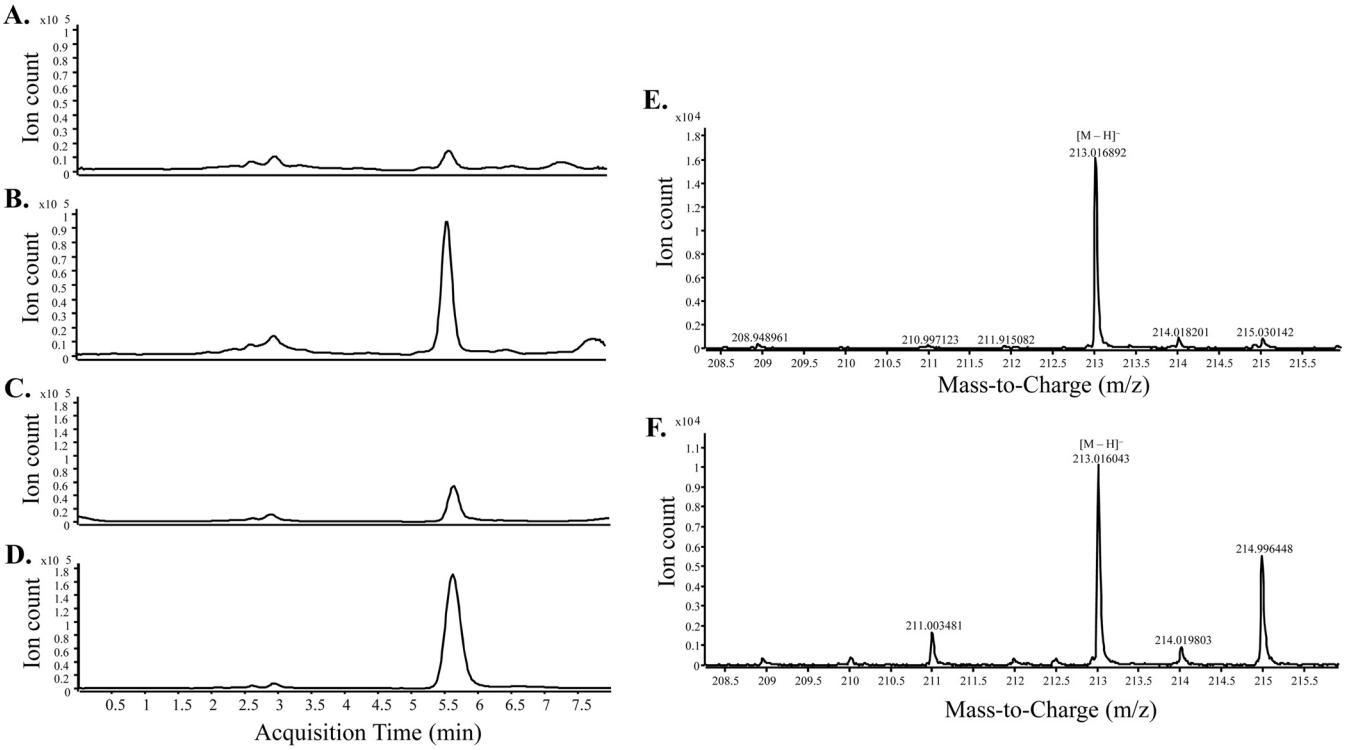

FIG 3 *In vitro* production of DXP (5.7 min) from Ru5P by RibB(G108S) and YajO. (A to D) Chromatograms for DXP produced *in vivo* by yajO (A) and RibB(G108S) (C); the data in panels B and D, respectively, represent the results determined with the same samples spiked with 4 μM DXP to confirm the retention time for DXP. (E and F) Mass spectra for a DXP standard (E) and DXP produced by RibB(G108S) (F).

way engineering alongside native levels of Dxs, the host strain was changed from strain Δ*dxs*MB to *E. coli* BL21(DE3). In addition, we selected the candidate biofuel α-bisabolene as the target sesquiterpene product. To assess synergy between DXP pathway engineering and nDXP routes, we constructed vectors for expression of bisabolene synthase (AgBIS) together with DXP pathway enzymes that have previously been shown to limit pathway flux, namely, those encoded by *ispD*, *ispF*, *idi*, and *ispA* (31). Expression of *yajO* or *ribB*(G108S) alongside plasmid pBbA1k-*AgBIS-ispDF-idi* yielded a 2-to-3-fold improvement in bisabolene titers compared to those seen with an *rfp* control vector (Fig. 4A). Having previously tested fusions of Dxs/Dxr for DXP pathway engineering and found no benefit in terms of the bisabolene titer (data not shown), we constructed nDXP/Dxr fusions, using the native *ispC* gene encoding Dxr, to determine if pathway flux could be enhanced. In comparisons of several fusions in which different orders of the proteins and the peptide linkers were used, *ispC*-G2-*ribB*(G108S), where G2 corresponds to a GSGGSG linker, yielded the highest increase in the bisabolene titer (see Fig. S3 in the supplemental material).

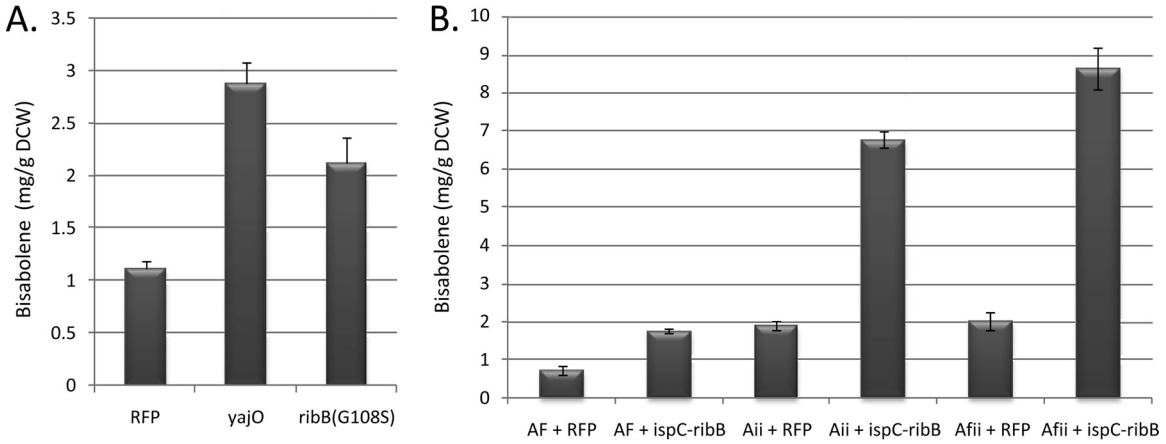

FIG 4 Bisabolene production via the DXP pathway in *E. coli* using nDXP genes. (A) Expression of *rfp*, *yajO*, or *ribB*(*G108S*) combined with pBbA1k-*AgBIS-ispDF-idi*. (B) Expression of *rfp* or an *ispC*-$(GSG)_2$-*ribB*(*G108S*) fusion (ispC-ribB) coupled with pBbA1k-*AgBIS-ispA* (AF), pBbA1k-*AgBIS-ispDF-idi* (Aii), or pBbA1k-*AgBIS-ispA-ispDF-idi* (Afii).

TABLE 2 Measurement of DXP pathway intermediates in two *E. coli* strains engineered for bisabolene production[a]

E. coli strain	Concn (μM)					
	DXP	MEP	CDP-ME	MEcPP	HMBPP	IPP/DMAPP
Afii + RFP	1.13 (0.62)	0.00	0.00	13.9 (5.2)	0.00	0.00
Afii + Dxr-RibB	0.00	0.15 (0.01)	0.43 (0.06)	38.7 (13.3)	0.00	0.00

[a] Vectors harboring *rfp* or an *ispC*-G2-*ribB*(G108S) fusion (Dxr-RibB) were coupled with pBbA1k-*AgBIS-ispA-ispDF-idi* (Afii). Concentrations are normalized to culture OD; standard deviations from three cultures are shown in parentheses. CDP-ME, 4-diphosphocytidyl-2-C-methyl-D-erythritol; HMBPP, (*E*)-4-hydroxy-3-methyl-but-2-enyl pyrophosphate.

To further investigate the *ispC*-G2-*ribB*(G108S) fusion, we first coupled it with three different vectors harboring AgBIS and DXP pathway genes (Fig. 4B). The overall bisabolene titer as well as the increase over control levels became progressively higher as the *ispC*-G2-*ribB*(G108S) fusion was coupled with progressively engineered DXP pathway vectors. Coupling pTrc99A-*ispC*-G2-*ribB*(G108S) with pBbA1k-*AgBIS-ispA-ispDF-idi* (Afii) yielded a 4.3-fold increase over the levels of a control strain in which Afii was coupled with *rfp*. To determine how this affected DXP pathway flux, we measured pathway intermediates in these two strains (Table 2). In the RFP control strain, only two metabolites were detected, DXP and MEcPP (2-C-methyl-D-erythritol 2,4-cyclophosphate), the latter being the substrate for IspG, which is known to be kinetically slow (32). In the equivalent strain harboring pTrc99A-*ispC*-G2-*ribB*(G108S), DXP did not accumulate to detectable levels whereas MEcPP levels were almost 3-fold higher than those seen with the *rfp* strain. Together, these data suggest that fusion of Dxr to RibB increases flux through the pathway, circumvents accumulation of DXP, and results in increased accumulation of MEcPP, implicating IspG as a suitable target for further engineering studies.

DISCUSSION

Metabolic engineering of terpene production in microbes or plants usually entails overexpression of key enzymes in the mevalonate or DXP precursor pathways (33). Dxs is an important control point in the DXP pathway as demonstrated by the fact that overexpression has increased terpene titers in several species (34, 35). However, the benefit gained by increasing Dxs levels is somewhat limited by regulatory mechanisms that can occur posttranscriptionally (36, 37), for example, via feedback inhibition by prenyl phosphates (12, 38). The nDXP enzymes described here provide alternative routes to DXP accumulation that may facilitate terpene pathway engineering by circumventing regulatory issues and also carbon loss associated with the Dxs-catalyzed reaction (Fig. 1). Additional benefits may arise depending on the carbon source provided to the production host; for example, nDXP expression may benefit *E. coli* grown on mixed sugars derived from hemicellulosic feedstocks by shunting the pentose fraction more directly to the DXP pathway following conversion to Ru5P. Alternatively, engineering nDXP in plants and algae could provide a more direct link from carbon fixation (Ru5P in the Calvin cycle) to the terpene pathway.

Calculation of the stoichiometric pathway efficiency, accounting for the cost of NADPH and ATP utilized together with the molar product yield (10), reveals that the nDXP route is more efficient not only from pentoses but also from glucose. Conversion of glucose 6-phosphate to Ru5P via the oxidative phase of the pentose phosphate pathway generates 2 NADPHs, which may serve as cofactors in the DXP pathway. The resulting theoretical pathway efficiency of production of terpenes from glucose via the nDXP route is close to the maximum theoretical biochemical yield (0.309 g bisabolene per gram of glucose versus 0.324 g bisabolene per gram of glucose, respectively).

Our approach to screening for nDXP genes entailed growth on xylose as the sole carbon source. Interestingly, mutations in the *aceE* gene, previously shown to convert pyruvate and glyceraldehyde to DX (25), were not encountered in any of the first 50 mevalonate prototrophs isolated, perhaps indicating that the mutant RibB route for synthesis of DXP is more efficient than the mutant AceE route in the presence of high Ru5P levels. Overexpression of *ribB*(G108S) also enabled normal growth in the absence of mevalonate of strain Δ*dxs*MB on glucose, while overexpression of *yajO* enabled growth only on xylose, suggesting that YajO may require higher Ru5P levels to support growth due to kinetic limitations.

The remaining genomic mutation found to complement growth in strain Δ*dxs*MB, encoding GatC(D296A), was not investigated further. However, since GatC can function as an ATP-independent xylose transporter, it seems likely that the main benefit from the mutation may be increased uptake of xylose (27), perhaps increasing the Ru5P concentration to the point where native levels of YajO can generate sufficient DXP to sustain a low level of growth.

Two mutations in *ribB* have been recently found to complement Δ*dxs* in *E. coli* grown on LB medium (20); here we have identified one of the same mutations (G108S) along with 6 others (T88I, S89R, G92D, T106I, V109I, and M182I) that complement Δ*dxs* in *E. coli* grown on xylose and have elucidated the reaction catalyzed. Nuclear magnetic resonance (NMR) and crystal structures have been solved for RibB from *E. coli* and other species, and a reaction mechanism has been proposed for conversion of Ru5P to the riboflavin precursor DHBP (39–42). Several of the RibB mutations that enable production of DXP are at or close to catalytically important residues; for example, G108 is conserved among RibB proteins from diverse sources and is suggested by NMR studies to play a role in substrate binding (40), while crystal structure analysis suggests that the presence of a nonglycine residue at this critical turn would result in a sterically strained conformation (41). Since the reaction mechanism proposed for wt RibB involves the generation of 1-deoxy intermediates, one possibility is that the mutations result in termination of the reaction prior to the proposed carbon rearrangement and elimination of formate (26, 41). However, the exact mechanism and means of reduction remain unknown and require further investigation.

Although the reaction catalyzed by the mutant RibB enzyme is unusual, it is not unique; YajO from *E. coli* can also catalyze formation of DXP from Ru5P, albeit less efficiently. YajO was origi-

nally annotated as a putative xylose reductase, but little evidence was found for this activity *in vitro*, and *E. coli* is known to utilize the alternative xylose isomerase route for xylose assimilation (14). YajO is now most often annotated as a 2-carboxybenzaldehyde reductase based on detection of this activity *in vitro*, but since *E. coli* is not known for polyaromatic hydrocarbon degradation, the true biological function for the enzyme remains unknown (14). It is tempting to speculate that YajO may play a role in biosynthesis of DXP (which, besides its role in the isoprenoid pathway, serves as a precursor to thiamine) under conditions of thiamine starvation. Since Dxs requires thiamine pyrophosphate as a cofactor, thiamine starvation would leave cells in a state where synthesis of DXP for *de novo* thiamine (and isoprenoid) biosynthesis would not be possible. YajO could serve a role in low-level DXP biosynthesis from Ru5P to kick-start thiamine biosynthesis and, consequently, Dxs. As mentioned, *yajO* is located next to *dxs* on the *E. coli* genome, and *thiL*, which encodes the final enzyme in the thiamine biosynthetic pathway, is situated less than 1 kb downstream.

Having demonstrated the utility of nDXP genes in engineering terpene production in *E. coli*, we investigated the use of protein fusions to further increase yields of the candidate biofuel bisabolene. The use of fusions or scaffolds has been demonstrated to increase pathway flux in several situations, including terpene pathway engineering (43, 44). Having found that Dxs/Dxr fusions (in either orientation, with both using GSGGSG linkers) did not yield an increase in the bisabolene titer, we tested Dxr/nDXP fusions where the gene corresponding to nDXP was either *yajO* or *ribB*(G108S) and found that *ispC*-G2-*ribB*(G108S) yielded a 4.3 improvement in bisabolene production over the level seen with the control strain. The fact that DXP accumulation in this strain was below the limit of detection suggests that the metabolic flux from Ru5P to MEP (2C-methyl-D-erythritol 4-phosphate) is efficient. However, extensive further engineering of the DXP pathway will be required to achieve terpene yields close to the theoretical maximum in *E. coli*. Our analysis of DXP pathway intermediates, together with previously published studies, suggests that IspG is a key pathway bottleneck that should be addressed together with the genes expressed here (45, 46). We are also currently investigating the utility of the nDXP genes and fusions in plant hosts where a direct link from carbon fixation to biofuel production presents an attractive opportunity.

ACKNOWLEDGMENTS

J.D.K. has a financial interest in Amyris and Lygos.

The work conducted through the Joint BioEnergy Institute was supported by the Office of Science, Office of Biological and Environmental Research, of the U.S. Department of Energy under contract no. DE-AC02-05CH11231. The work conducted through the University of California at Berkeley was funded through the U.S. Department of Energy ARPA-E PETRO program, under grant no. DE-AR0000209.

REFERENCES

1. **Pérez-Gil J, Rodríguez-Concepción M.** 2013. Metabolic plasticity for isoprenoid biosynthesis in bacteria. Biochem J **452:**19–25.
2. **Tippmann S, Chen Y, Siewers V, Nielsen J.** 2013. From flavors and pharmaceuticals to advanced biofuels: production of isoprenoids in Saccharomyces cerevisiae. Biotechnol J **8:**1435–1444. http://dx.doi.org/10.1002/biot.201300028.
3. **Boucher Y, Doolittle WF.** 2000. The role of lateral gene transfer in the evolution of isoprenoid biosynthesis pathways. Mol Microbiol **37:**703–716. http://dx.doi.org/10.1046/j.1365-2958.2000.02004.x.
4. **Skjånes K, Rebours C, Lindblad P.** 2013. Potential for green microalgae to produce hydrogen, pharmaceuticals and other high value products in a combined process. Crit Rev Biotechnol **33:**172–215. http://dx.doi.org/10.3109/07388551.2012.681625.
5. **Ye VM, Bhatia SK.** 2012. Pathway engineering strategies for production of beneficial carotenoids in microbial hosts. Biotechnol Lett **34:**1405–1414. http://dx.doi.org/10.1007/s10529-012-0921-8.
6. **Onrubia M, Cusido RM, Ramirez K, Hernandez-Vazquez L, Moyano E, Bonfill M, Palazon J.** 2013. Bioprocessing of plant in vitro systems for the mass production of pharmaceutically important metabolites: paclitaxel and its derivatives. Curr Med Chem **20:**880–891. http://dx.doi.org/10.2174/0929867311320070004.
7. **Paddon CJ, Westfall PJ, Pitera DJ, Benjamin K, Fisher K, McPhee D, Leavell MD, Tai A, Main A, Eng D, Polichuk DR, Teoh KH, Reed DW, Treynor T, Lenihan J, Fleck M, Bajad S, Dang G, Dengrove D, Diola D, Dorin G, Ellens KW, Fickes S, Galazzo J, Gaucher SP, Geistlinger T, Henry R, Hepp M, Horning T, Iqbal T, Jiang H, Kizer L, Lieu B, Melis D, Moss N, Regentin R, Secrest S, Tsuruta H, Vazquez R, Westblade LF, Xu L, Yu M, Zhang Y, Zhao L, Lievense J, Covello PS, Keasling JD, Reiling KK, Renninger NS, Newman JD.** 2013. High-level semi-synthetic production of the potent antimalarial artemisinin. Nature **496:**528–532. http://dx.doi.org/10.1038/nature12051.
8. **Du J, Shao Z, Zhao H.** 2011. Engineering microbial factories for synthesis of value-added products. J Ind Microbiol Biotechnol **38:**873–890. http://dx.doi.org/10.1007/s10295-011-0970-3.
9. **Li H, Cann AF, Liao JC.** 2010. Biofuels: biomolecular engineering fundamentals and advances. Annu Rev Chem Biomol Eng **1:**19–36. http://dx.doi.org/10.1146/annurev-chembioeng-073009-100938.
10. **Dugar D, Stephanopoulos G.** 2011. Relative potential of biosynthetic pathways for biofuels and bio-based products. Nat Biotechnol **29:**1074–1078. http://dx.doi.org/10.1038/nbt.2055.
11. **Scheller HV, Ulvskov P.** 2010. Hemicelluloses. Annu Rev Plant Biol **61:**263–289. http://dx.doi.org/10.1146/annurev-arplant-042809-112315.
12. **Banerjee A, Wu Y, Banerjee R, Li Y, Yan H, Sharkey TD.** 2013. Feedback inhibition of deoxy-D-xylulose-5-phosphate synthase regulates the methylerythritol 4-phosphate pathway. J Biol Chem **288:**16926–16936. http://dx.doi.org/10.1074/jbc.M113.464636.
13. **Richter G, Volk R, Krieger C, Lahm HW, Rothlisberger U, Bacher A.** 1992. Biosynthesis of riboflavin: cloning, sequencing, and expression of the gene coding for 3,4-dihydroxy-2-butanone 4-phosphate synthase of Escherichia coli. J Bacteriol **174:**4050–4056.
14. **Ko J, Kim I, Yoo S, Min B, Kim K, Park C.** 2005. Conversion of methylglyoxal to acetol by Escherichia coli aldo-keto reductases. J Bacteriol **187:**5782–5789. http://dx.doi.org/10.1128/JB.187.16.5782-5789.2005.
15. **Martin VJ, Pitera DJ, Withers ST, Newman JD, Keasling JD.** 2003. Engineering a mevalonate pathway in Escherichia coli for production of terpenoids. Nat Biotechnol **21:**796–802. http://dx.doi.org/10.1038/nbt833.
16. **Datsenko KA, Wanner BL.** 2000. One-step inactivation of chromosomal genes in Escherichia coli K-12 using PCR products. Proc Natl Acad Sci U S A **97:**6640–6645. http://dx.doi.org/10.1073/pnas.120163297.
17. **Rose MD, Fink GR.** 1987. KAR1, a gene required for function of both intranuclear and extranuclear microtubules in yeast. Cell **48:**1047–1060. http://dx.doi.org/10.1016/0092-8674(87)90712-4.
18. **Schlösser T, Schmidt G, Stahmann KP.** 2001. Transcriptional regulation of 3,4-dihydroxy-2-butanone 4-phosphate synthase. Microbiology **147:**3377–3386.
19. **Baidoo EE, Xiao Y, Dehesh K, Keasling JD.** 2014. Metabolite profiling of plastidial deoxyxylulose-5-phosphate pathway intermediates by liquid chromatography and mass spectrometry. Methods Mol Biol **1153:**57–76. http://dx.doi.org/10.1007/978-1-4939-0606-2_5.
20. **Perez-Gil J, Uros EM, Sauret-Gueto S, Lois LM, Kirby J, Nishimoto M, Baidoo EE, Keasling JD, Boronat A, Rodriguez-Concepcion M.** 2012. Mutations in Escherichia coli aceE and ribB genes allow survival of strains defective in the first step of the isoprenoid biosynthesis pathway. PLoS One **7:**e43775. http://dx.doi.org/10.1371/journal.pone.0043775.
21. **Paradise EM, Kirby J, Chan R, Keasling JD.** 2008. Redirection of flux through the FPP branch-point in Saccharomyces cerevisiae by down-regulating squalene synthase. Biotechnol Bioeng **100:**371–378. http://dx.doi.org/10.1002/bit.21766.
22. **Peralta-Yahya PP, Ouellet M, Chan R, Mukhopadhyay A, Keasling JD, Lee TS.** 2011. Identification and microbial production of a terpene-based

advanced biofuel. Nat Commun **2:**483. http://dx.doi.org/10.1038/ncomms1494.
23. **Lee TS, Krupa RA, Zhang F, Hajimorad M, Holtz WJ, Prasad N, Lee SK, Keasling JD.** 2011. BglBrick vectors and datasheets: a synthetic biology platform for gene expression. J Biol Eng **5:**12. http://dx.doi.org/10.1186/1754-1611-5-12.
24. **Li MZ, Elledge SJ.** 2007. Harnessing homologous recombination in vitro to generate recombinant DNA via SLIC. Nat Methods **4:**251–256. http://dx.doi.org/10.1038/nmeth1010.
25. **Sauret-Güeto S, Urós EM, Ibáñez E, Boronat A, Rodríguez-Concepción M.** 2006. A mutant pyruvate dehydrogenase E1 subunit allows survival of Escherichia coli strains defective in 1-deoxy-D-xylulose 5-phosphate synthase. FEBS Lett **580:**736–740. http://dx.doi.org/10.1016/j.febslet.2005.12.092.
26. **Bacher A, Eberhardt S, Fischer M, Kis K, Richter G.** 2000. Biosynthesis of vitamin b2 (riboflavin). Annu Rev Nutr **20:**153–167. http://dx.doi.org/10.1146/annurev.nutr.20.1.153.
27. **Nduko JM, Matsumoto K, Ooi T, Taguchi S.** 2014. Enhanced production of poly(lactate-co-3-hydroxybutyrate) from xylose in engineered Escherichia coli overexpressing a galactitol transporter. Appl Microbiol Biotechnol **98:**2453–2460. http://dx.doi.org/10.1007/s00253-013-5401-0.
28. **Nobelmann B, Lengeler JW.** 1996. Molecular analysis of the gat genes from Escherichia coli and of their roles in galactitol transport and metabolism. J Bacteriol **178:**6790–6795.
29. **Lawhorn BG, Gerdes SY, Begley TP.** 2004. A genetic screen for the identification of thiamin metabolic genes. J Biol Chem **279:**43555–43559. http://dx.doi.org/10.1074/jbc.M404284200.
30. **Hecht S, Eisenreich W, Adam P, Amslinger S, Kis K, Bacher A, Arigoni D, Rohdich F.** 2001. Studies on the nonmevalonate pathway to terpenes: the role of the GcpE (IspG) protein. Proc Natl Acad Sci U S A **98:**14837–14842. http://dx.doi.org/10.1073/pnas.201399298.
31. **Yuan LZ, Rouviere PE, Larossa RA, Suh W.** 2006. Chromosomal promoter replacement of the isoprenoid pathway for enhancing carotenoid production in E. coli. Metab Eng **8:**79–90. http://dx.doi.org/10.1016/j.ymben.2005.08.005.
32. **Xu W, Lees NS, Adedeji D, Wiesner J, Jomaa H, Hoffman BM, Duin EC.** 2010. Paramagnetic intermediates of (E)-4-hydroxy-3-methylbut-2-enyl diphosphate synthase (GcpE/IspG) under steady-state and pre-steady-state conditions. J Am Chem Soc **132:**14509–14520. http://dx.doi.org/10.1021/ja101764w.
33. **Vickers CE, Bongers M, Liu Q, Delatte T, Bouwmeester H.** 2014. Metabolic engineering of volatile isoprenoids in plants and microbes. Plant Cell Environ **37:**1753–1775. http://dx.doi.org/10.1111/pce.12316.
34. **Kim SW, Keasling JD.** 2001. Metabolic engineering of the nonmevalonate isopentenyl diphosphate synthesis pathway in Escherichia coli enhances lycopene production. Biotechnol Bioeng **72:**408–415. http://dx.doi.org/10.1002/1097-0290(20000220)72:4<408::AID-BIT1003>3.0.CO;2-H.
35. **Muñoz-Bertomeu J, Arrillaga I, Ros R, Segura J.** 2006. Up-regulation of 1-deoxy-D-xylulose-5-phosphate synthase enhances production of essential oils in transgenic spike lavender. Plant Physiol **142:**890–900. http://dx.doi.org/10.1104/pp.106.086355.
36. **Cordoba E, Salmi M, Leon P.** 2009. Unravelling the regulatory mechanisms that modulate the MEP pathway in higher plants. J Exp Bot **60:**2933–2943. http://dx.doi.org/10.1093/jxb/erp190.
37. **Wright LP, Rohwer JM, Ghirardo A, Hammerbacher A, Ortiz-Alcaide M, Raguschke B, Schnitzler JP, Gershenzon J, Phillips MA.** 2014. Deoxyxylulose 5-phosphate synthase controls flux through the methylerythritol 4-phosphate pathway in Arabidopsis. Plant Physiol **165:**1488–1504. http://dx.doi.org/10.1104/pp.114.245191.
38. **Ghirardo A, Wright LP, Bi Z, Rosenkranz M, Pulido P, Rodriguez-Concepcion M, Niinemets U, Bruggemann N, Gershenzon J, Schnitzler JP.** 2014. Metabolic flux analysis of plastidic isoprenoid biosynthesis in poplar leaves emitting and nonemitting isoprene. Plant Physiol **165:**37–51. http://dx.doi.org/10.1104/pp.114.236018.
39. **Steinbacher S, Schiffmann S, Richter G, Huber R, Bacher A, Fischer M.** 2003. Structure of 3,4-dihydroxy-2-butanone 4-phosphate synthase from Methanococcus jannaschii in complex with divalent metal ions and the substrate ribulose 5-phosphate: implications for the catalytic mechanism. J Biol Chem **278:**42256–42265. http://dx.doi.org/10.1074/jbc.M307301200.
40. **Kelly MJ, Ball LJ, Krieger C, Yu Y, Fischer M, Schiffmann S, Schmieder P, Kuhne R, Bermel W, Bacher A, Richter G, Oschkinat H.** 2001. The NMR structure of the 47-kDa dimeric enzyme 3,4-dihydroxy-2-butanone-4-phosphate synthase and ligand binding studies reveal the location of the active site. Proc Natl Acad Sci U S A **98:**13025–13030. http://dx.doi.org/10.1073/pnas.231323598.
41. **Liao DI, Calabrese JC, Wawrzak Z, Viitanen PV, Jordan DB.** 2001. Crystal structure of 3,4-dihydroxy-2-butanone 4-phosphate synthase of riboflavin biosynthesis. Structure **9:**11–18. http://dx.doi.org/10.1016/S0969-2126(00)00550-5.
42. **Volk R, Bacher A.** 1991. Biosynthesis of riboflavin. Studies on the mechanism of L-3,4-dihydroxy-2-butanone 4-phosphate synthase. J Biol Chem **266:**20610–20618.
43. **Dueber JE, Wu GC, Malmirchegini GR, Moon TS, Petzold CJ, Ullal AV, Prather KL, Keasling JD.** 2009. Synthetic protein scaffolds provide modular control over metabolic flux. Nat Biotechnol **27:**753–759. http://dx.doi.org/10.1038/nbt.1557.
44. **Brodelius M, Lundgren A, Mercke P, Brodelius PE.** 2002. Fusion of farnesyldiphosphate synthase and epi-aristolochene synthase, a sesquiterpene cyclase involved in capsidiol biosynthesis in Nicotiana tabacum. Eur J Biochem **269:**3570–3577. http://dx.doi.org/10.1046/j.1432-1033.2002.03044.x.
45. **Rivasseau C, Seemann M, Boisson AM, Streb P, Gout E, Douce R, Rohmer M, Bligny R.** 2009. Accumulation of 2-C-methyl-D-erythritol 2,4-cyclodiphosphate in illuminated plant leaves at supraoptimal temperatures reveals a bottleneck of the prokaryotic methylerythritol 4-phosphate pathway of isoprenoid biosynthesis. Plant Cell Environ **32:**82–92. http://dx.doi.org/10.1111/j.1365-3040.2008.01903.x.
46. **Zhou K, Zou R, Stephanopoulos G, Too HP.** 2012. Metabolite profiling identified methylerythritol cyclodiphosphate efflux as a limiting step in microbial isoprenoid production. PLoS One **7:**e47513. http://dx.doi.org/10.1371/journal.pone.0047513.